3D-Ising like ferromagnetism in skyrmionic-bubbles host infinite-layer La$_{0.825}$Sr$_{0.175}$MnO$_3$ manganite perovskite

Jeetendra Kumar Tiwari, Harish Chandr Chauhan, Birendra Kumar and Subhasis Ghosh

School of Physical Sciences, Jawaharlal Nehru University, New Delhi 110067, India

E-mail: subhasis.ghosh.jnu@gmail.com

Abstract
The critical behavior of infinite-layer La$_{0.825}$Sr$_{0.175}$MnO$_3$ of Ruddlesden–Popper series manganite has been studied around the transition temperature (T_C). To reveal the universality class that explains the critical behavior in La$_{0.825}$Sr$_{0.175}$MnO$_3$ several methods, such as modified Arrott plots, Kouvel–Fisher, entropy and critical isotherm analysis have been employed. The critical exponent δ for infinite-layer is obtained independently from critical magnetization isotherm and found to satisfy the Widom scaling relation $\delta = 1 + \gamma/\beta$. The universality class of the critical phenomenon in infinite-layer La$_{0.825}$Sr$_{0.175}$MnO$_3$ manganite can be explained with the help of renormalization group theory approach for three dimensional (3D) systems. We have shown that a short-range 3D-Ising type interaction is responsible for ferromagnetic and second-order phase transition to paramagnetic phase.

Keywords: critical phenomena, critical exponents, magnetic phase transitions, entropy, magnetic anisotropy, Landau theory

(Some figures may appear in colour only in the online journal)

1. Introduction

Different topologically equivalent spin textures, such as skyrmions and magnetic-bubbles are being investigated extensively in different magnetic materials. Skyrmions are generally observed in non-centrosymmetric B20 materials, such as MnSi, Cu$_2$OSeO$_3$, FeGe etc [1–4], due to antisymmetric Dzyaloshinskii–Moriya (DM) interaction. Now, it is highly desirable to explore new materials as a host for these topologically equivalent spin textures to extend the practical applications in spintronics. Rather unexpectedly skyrmion has been observed in manganites which are centrosymmetric materials and have been extensively studied in the past due to colossal magnetoresistance (CMR) [5–9]. In B20 materials (MnSi, Cu$_2$OSeO$_3$, FeGe etc) skyrmions are stabilized due to the competition between symmetric exchange interaction and antisymmetric DM interaction [2]. Hence, short-range interaction is responsible for topological spin textures [2]. However, short-range DM interaction cannot exist in the absence of

non-centrosymmetry, raising an important question regarding the origin of interaction responsible for topological spin textures in manganites. Though it has been conjectured that dipole-dipole interaction is responsible for skyrmion in manganites [10], but the role of exchange interaction cannot be ruled out. Moreover, the skyrmion phase observed at relatively higher temperature (95–100 K) [11], so it can be doubted how only dipole-dipole interaction could be responsible for skyrmion in these materials. In this context, the important questions are— what is the range of interaction responsible for the formation and stability of skyrmion in manganites? So, a detailed critical analysis of phase transition in these materials is needed to understand the universality class, which defines the range and dimensionality of the interaction responsible for different phases in materials. A particular universality class allows us to understand the fundamental physics such as range and dimensionality of the magnetic interaction for a second-order phase transition. Though, critical behavior of La$_{1-x}$Sr$_x$MnO$_3$ with different concentration ($x = 0.125$, 0.2, 0.25, 0.3)

of strontium (Sr) has been extensively studied [12–21], but most of the results on the range and type of interactions in manganites are incoherent and ambiguous. For example all possible universality classes, such as long-range mean field ($x = 0.2$ and 0.3) [12–14], short-range 3D-Heisenberg ($x = 0.125$ and 0.3) [15, 16] or 3D-Ising ($x = 0.2$, 0.3 and 0.25) [17–21] have been proposed to explain critical behavior in $La_{1-x}Sr_xMnO_3$. Initially, it was expected that mean field based long-range model would explain the interaction in $La_{1-x}Sr_xMnO_3$ in which effective ferromagnetism is induced by the double exchange mechanism [12–14]. Later on, Furukawa and Motome showed that the universality class of the double exchange ferromagnetic materials are consistent with that of short-range models instead of long-range model [22]. Presence of large magnetic anisotropy may lead to the 3D-Ising type interaction instead of a 3D-Heisenberg interaction [20]. The parent compound $LaMnO_3$ is antiferromagnet and found to have 3D-Heisenberg [23, 24] like short-range interaction. In the present study, we have chosen centrosymmetric, anisotropic infinite-layer $La_{0.825}Sr_{0.175}MnO_3$, hereafter referred to as LSMO, of Ruddlesden–Popper (RP) series. We have selected this particular composition (La is replaced with 17.5% Sr) because of the recently observed skyrmionic-bubbles in LSMO despite the absence of DM interaction due to centrosymmetric crystal structure [11]. The infinite-layer $La_{1-x}Sr_xMnO_3$ perovskite manganites are $n = \infty$ member of RP series $(La,Sr)_{n+1}Mn_nO_{3n+1}$ [25]. The infinite-layer has continuous stacking of perovskite structure with a 3D array of corner-sharing MnO_6 octahedrons. Fan *et al* [26] have studied this particular composition ($La_{0.825}Sr_{0.175}MnO_3$) and claimed that it belongs to mean field class based on very limited data without any detailed critical analysis. However, it is beyond a doubt that phase transition in these class of materials cannot be explained by mean field model [17–21, 27]. This paper aims to establish a complete understanding of the critical behavior of infinite-layer LSMO to find out the type and range of interaction responsible for ferromagnetic phases. Before critical analysis, we have first ensured the order of phase transition using entropy and Landau analysis, keeping in view of some reports of first order transition in $La_{1-x}Ca_xMnO_3$ for $x = 0.3$, 0.33 [28, 29]. We have studied the critical behavior of the sample around T_C using high precision magnetic measurements over a wide range of magnetic field and temperature.

2. Experimental details

Monophasic polycrystalline sample of infinite-layer $La_{0.825}Sr_{0.175}MnO_3$ was prepared through conventional solid state reaction method [30] using high purity La_2O_3 (Sigma Aldrich 99.99%), $SrCO_3$ (Alfa Aesar 99.995%) and MnO_2 (Alfa Aesar 99.997%). Stoichiometric ratio of La_2O_3 (pre-fired at 1000 °C for 12 h), $SrCO_3$ (dried in air at 150 °C for 12 h) and MnO_2 were thoroughly ground together and calcined at different temperatures 1150 °C, 1250 °C, 1350 °C for 60 h followed by intermediate grinding. The LSMO sample was calcined for 20 h at each temperature. The sample was then reground, pressed into pellet and sintered at 1400 °C

for 48 h. The final step was repeated until the single phase of LSMO sample is achieved. The phase purity and crystal structure of the sample were confirmed by powder x-ray diffraction (XRD) (Rigaku miniflex 600-x-ray diffractometer with Cu-K$_\alpha$ radiation) at room temperature. The high precision magnetic measurements were carried out using physical properties measurement system (PPMS) by three different methods, (i) field cooled (FC) temperature scans in the presence of magnetic field; the infinite-layer LSMO sample was cooled from room temperature to the desired low temperature. Finally, the temperature-dependent magnetization data was recorded during heating. (ii) Zero field cooled (ZFC) temperature scans; the sample was brought at low temperature and then by applying magnetic field the temperature-dependent magnetization data was recorded during heating. (iii) ZFC magnetic field scans; the sample was brought at the various required temperatures and held until the thermal equilibrium was reached. First quadrant magnetization (M–H) data were collected in the temperature range 262–300 K ($\Delta T = 2$ K) with the applied field step of 10 mT from 0 mT to 500 mT and above 500 mT the step size was increased to 200 mT and data was collected up to 7 T for exact analysis of phase transition and critical analysis of infinite-layer LSMO.

3. Results and discussion

3.1. X-ray diffraction analysis

Crystal structure and phase analysis of the room temperature XRD of infinite-layer LSMO has been investigated with the help of retveild refinement (figure 1). The LSMO sample is found to be a rhombohedral structure with R$\bar{3}$c space group. The lattice parameters are $a = b = 5.5354$ Å and $c = 13.3736$ Å. There is no peak corresponding to the secondary phase, confirming the single phase formation of the infinite-layer LSMO [31] (figure 1(a)). The schematic crystal structure of the infinite-layer LSMO (figure 1(b)) is made of MnO_6 octahedrons in which Mn atom lies in the center of the oxygen octahedron. The refinement results such as R_p (residuals for the pattern), R_{wp} (residuals for the weighted pattern), R_F (structure factor) and the goodness of fit etc are listed in the table 1.

3.2. Magnetic analysis

In order to study the phase transition between ferromagnetic (FM) to paramagnetic (PM) phases, we have carried out field-cooled (FC) and zero field-cooled (ZFC) temperature dependent magnetization (M–T) measurements of infinite-layer LSMO with an applied field of 50 mT (figure 2(a)). The FC curve shows a rapid change in the magnetization with decrease in temperature corresponding to the PM to FM transition. The magnetic transition temperature $T_C \approx 274$ K is obtained from the minimum of dM/dT (inset of figure 2(a)) [32]. A step down like behavior at ≈ 167 K, marked as T_S is due to a structural phase transition from rhombohedral to orthorhombic phase and not due to antiferromagnetic ordering
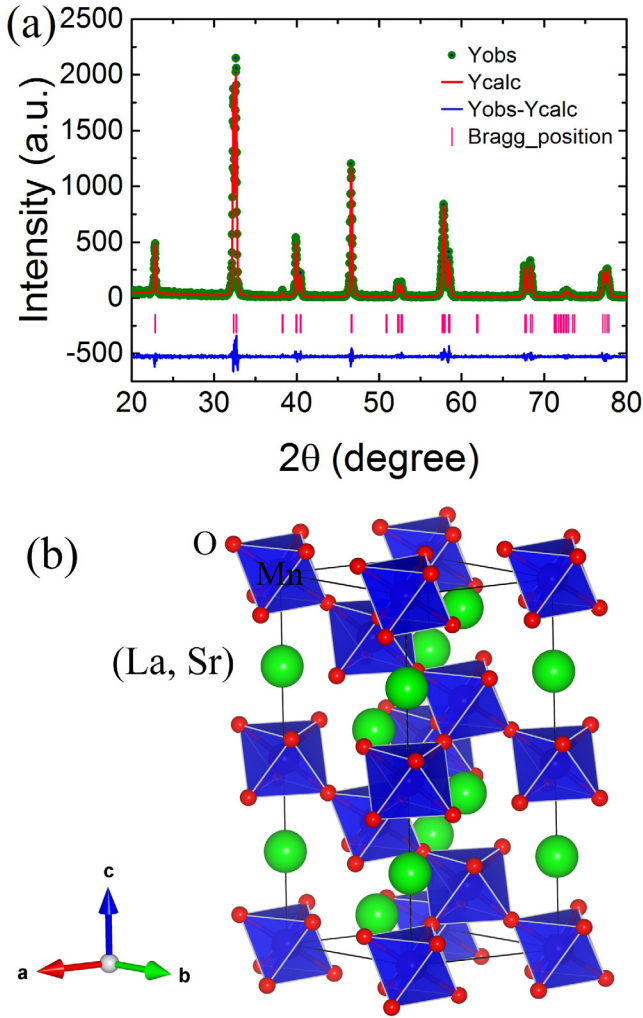
Figure 1. (a) Retveild refinement of the room temperature XRD and (b) crystal structure of the infinite-layer La$_{0.825}$Sr$_{0.175}$MnO$_3$, where different colors of the sphere represent the different atoms (red—oxygen, light green—(La, Sr) and blue—Mn).

Table 1. Room temperature structural parameters of infinite-layer LSMO obtained from retveild refinement.

Parameters	La$_{0.825}$Sr$_{0.175}$MnO$_3$
Symmetry	Rhombohedral
Space group	R$\bar{3}$c
$a = b$ (Å)	5.5354
c (Å)	13.3736
V (Å^3)	354.8789
R_p (%)	12.7
R_{wp} (%)	17.1
R_F (%)	2.80
χ^2 (%)	1.316

[31]. Figure 2(b) shows the M-H data of infinite-layer LSMO measured in the vicinity of T_C.

3.3. It is a second-order phase transition

It is extremely important to determine the order of phase transition from paramagnetic phase to ferromagnetic phase
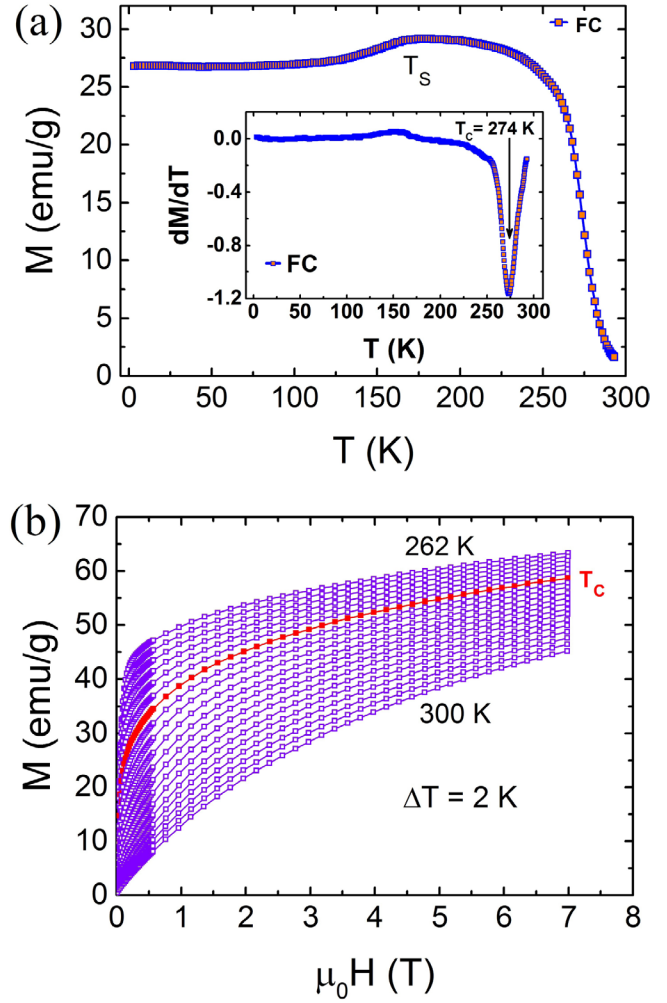

Figure 2. (a) FC of La$_{0.825}$Sr$_{0.175}$MnO$_3$ under an applied field of 50 mT. The inset shows the derivative of magnetization (dM/dT), where a minima was found at $\approx$274 K corresponding to T_C. (b) M–H data of infinite-layer LSMO recorded with an applied field of 0 to 7 Tesla at various temperatures ranging from 262 K to 300 K, $\Delta T = 2$ K.

as shown in figure 2. As mentioned before, there are some reports claiming that if Sr in La$_{1-x}$Sr$_x$MnO$_3$ is replaced with calcium (Ca), the magnetic transition is first-order [28, 29]. Hence before detailed critical analysis, one has to determine the order of phase transition unambiguously from two independent methods, such as entropy analysis [33–36] and Landau analysis [37].

3.3.1. Entropy analysis. Magnetic entropy change, $|\Delta S_M|$, of infinite-layer LSMO around T_C can be determined from isothermal magnetization data using Maxwell's thermodynamic relation [3, 38]:

$$\Delta S_M(\mu_0 H, T) = \int_0^{\mu_0 H} \left(\frac{\partial M(\mu_0 H, T)}{\partial T} \right)_H d(\mu_0 H), \quad (1)$$

where μ_0 is the permeability of vacuum, H is the applied magnetic field, M is the magnetization. Infinite layer perovskite manganites exhibit a very large magnetic entropy change around T_C [39–41] due to efficient ordering of spins [42]. Guo *et al* [43] suggested that the large $|\Delta S_M|$ in perovskite
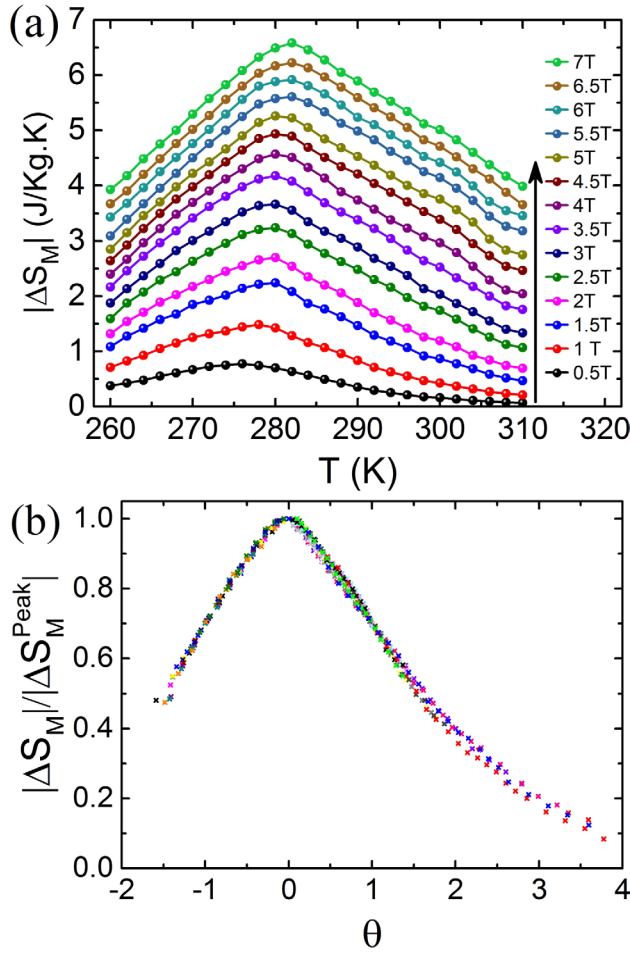
Figure 3. (a) Magnetic entropy change $|\Delta S_M|$ evolution versus temperature T at different applied magnetic fields. (b) the rescaled entropy curve in the field range 0.5 T–7 T.

compounds can be due to the spin-lattice coupling. The magnitude of the $|\Delta S_M|$ increases gradually with an increase in the applied magnetic field. A continuous nonmonotonic change of $|\Delta S_M|$ with temperature is an indication of the second-order phase transition around T_C, shown in figure 3(a). Further to ensure the order of phase transition of the infinite-layer LSMO, we have used the rescaling of $|\Delta S_M|$. The scaling of $|\Delta S_M|$ emphasize that if the LSMO sample exhibit a second-order phase transition, then all the rescaled $|\Delta S_M|$ curves must collapse onto a single universal curve [33–36]. Franco *et al* have shown theoretically the existence of such universal curve in case of second-order phase transition [33]. Different physical quantity can be scaled in the vicinity of a second-order transition [44] and the scaling relation for a magnetic system is given by [45]

$$\frac{H}{M^\delta} = h\left(\frac{\epsilon}{M^{1/\beta}}\right), \tag{2}$$

where $\epsilon = (T - T_C/T_C)$ is the reduced temperature, β and δ are the critical exponents for the magnetization behavior ($H = 0$, $\epsilon < 0$) and the critical isotherm ($\epsilon = 0$) respectively, and $h(x)$ is a scaling function ($x = \epsilon/M^{1/\beta}$). Systems belonging to the same universality class have same scaling

function $h(x)$ provided that the magnetization and magnetic field units are such that $h(0) = 1$ and $h(-1) = 0$, so equation (2) can be rewritten as

$$\frac{M}{|\epsilon|^\beta} = m_\pm\left(\frac{H}{|\epsilon|^\Delta}\right), \tag{3}$$

where $\Delta = \beta\delta$ is the gap exponent. From equations (1)–(3) $|\Delta S_M|$ can be expressed as

$$\Delta S_M/a_M = \pm|\epsilon|^{1-\alpha}\int_0^{H/|\epsilon|^\Delta} dx[\beta m \pm (x) - \Delta x m'_\pm(x)]$$
$$= |\epsilon|^{1-\alpha}\tilde{s}(\epsilon/H^{1/\Delta}) = H^{1-\alpha/\Delta}s(\epsilon/H^{1/\Delta}), \tag{4}$$

where $a_M = T_C^{-1}A^{\delta+1}B$, ($A$ and B are the critical amplitudes) and $s(x)$ is the scaling function ($x = \epsilon/H^{1/\Delta}$). If $|\Delta S_M|$ is rescaled by $a_M H^{(1-\alpha/)\Delta}$ and ϵ by a factor $H^{1/\Delta}$ the equation (4) implies that the experimental data would collapse onto the single curve [36]. A phenomenological way of doing this would be to normalize all the $|\Delta S_M|$ by the maximum value of the $|\Delta S_M|$ i.e. $|\Delta S_M^{peak}|$ which occurs at T_C. To rescale the temperature axis we need to choose a reference temperature such that $|\Delta S_M(T_r)|/|\Delta S_M^{peak}| \geqslant K$. Where, K is defined as the relative value of the entropy changes at two reference temperatures, K must have a value between $0 < K \leqslant 1$ [46]. We have chosen two reference temperatures $T_{r_1} < T_C$ and $T_{r_2} > T_C$ such that $|\Delta S_M(T_{r_1})|/|\Delta S_M^{peak}| = |\Delta S_M(T_{r_2})|/|\Delta S_M^{peak}| = 0.7$ and the rescaled temperature axis, say θ, is defined as

$$\theta = -(T - T_C)/(T_{r_1} - T_C), \ T \leqslant T_C$$
$$= (T - T_C)/(T_{r_2} - T_C), \ T > T_C. \tag{5}$$

Figure 3(b), shows the rescaled entropy curve in the field range 0.5 T–7 T. It can be noted that all the rescaled entropy curve collapses on a single universal curve, which confirms the second-order phase transition in infinite-layer LSMO.

3.3.2. Landau analysis. The magnetic free energy $F(M,T)$ of a ferromagnet can be expressed as a power series in terms of the order parameter M [47]

$$F(M,T) = F(0) + \frac{a_1(T)}{2}M^2 + \frac{a_3(T)}{4}M^4 + \frac{a_5(T)}{6}M^6 \tag{6}$$
$$+ ... - \mu_0 HM,$$

where $a_1(T)$, $a_3(T)$, and $a_5(T)$ are Landau coefficients. $F(M,T)$ allows us to determine the nature of the phase transition around T_C. The minimization of the thermodynamic potential $\partial F(M,T)/\partial M = 0$ gives the equilibrium condition, resulting

$$\mu_0 H = a_1(T)M + a_3(T)M^3 + a_5(T)M^5. \tag{7}$$

The Landau coefficients $a_1(T)$, $a_3(T)$, and $a_5(T)$ can be determined by equation (7). The temperature dependent Landau coefficients $a_1(T)$ and $a_3(T)$ permit us to differentiate the first-order and second-order phase transitions. The positive sign of $a_3(T)$ at T_C corresponds to the second-order and negative sign corresponds to the first-order phase transition [37]. The minima in $a_1(T)$ is correlated with the T_C of the infinite-layer
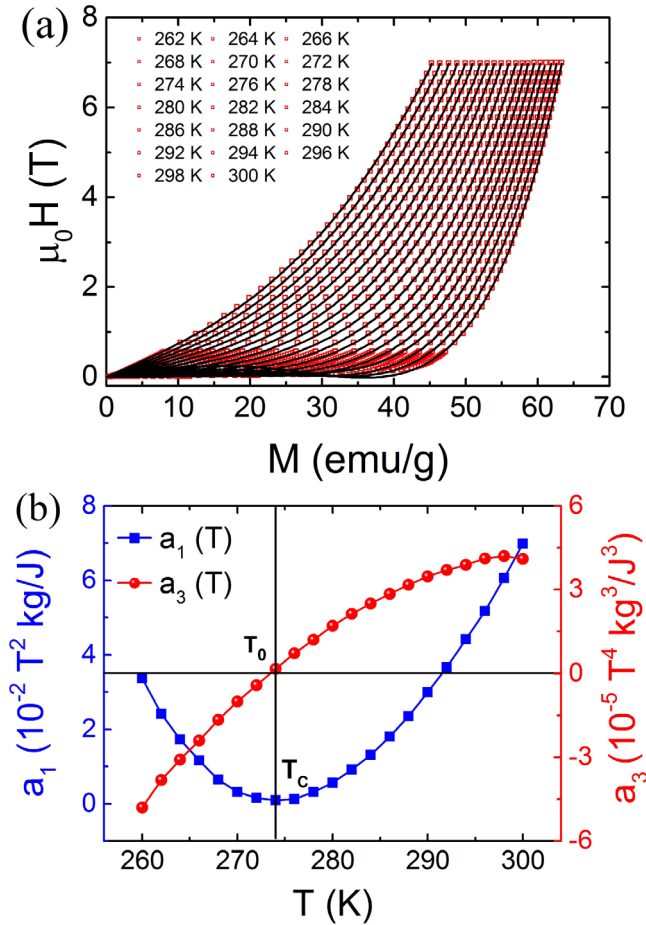
Figure 4. (a) Isothermal Magnetization curve at various temperatures. The solid lines show the fits to equation (7), (b) The temperature dependence of Landau coefficients $a_1(T)$, $a_3(T)$.

LSMO sample. While the coefficient $a_3(T)$ crosses zero at a second temperature, say T_0.

The Landau coefficients $a_1(T)$ and $a_3(T)$ were obtained by fitting the magnetic isotherms (figure 4(a)) using equation (7). The variation of Landau coefficients with temperature are shown in figure 4(b). It has been found that $a_3(T) > 0$ at T_C. This implies that infinite-layer LSMO exhibits a second-order phase transition near T_C (figure 4(b)).

3.4. Critical analysis and scaling

A particular universality class enables us to understand the mechanisms responsible for different types magnetic phases. There are predominantly five universality classes which define the phase transition in magnetic materials: (i) mean field model (ii) tricritical mean field model (iii) three dimensional (3D) Heisenberg model, (iv) 3D-Ising model, and (v) 3D-XY model. Generally, under long-range mean field approximation, T_C and critical exponents can be determined from Arrott plot (M^2 versus $\mu_0 H/M$) [48]. If the M–H data at different temperatures plotted as M^2 versus $\mu_0 H/M$ (Arrott plot) are not parallel, one has to go beyond mean field approximation. Hence long-range universality classes such as long-range mean field and long-range tricritical mean field can be
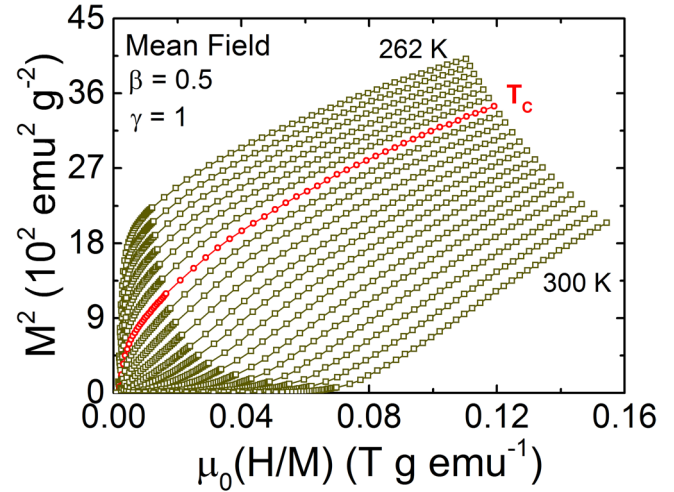

Figure 5. Arrott plot (M^2 versus $\mu_0 H/M$) of the M–H curves of infinite-layer LSMO measured at various temperatures ranging from 262 K to 300 K, $\Delta T = 2$ K.

ruled out. The Arrott plot of infinite-layer LSMO around T_C is shown in figure 5. The non-linear behavior of the Arrott plot even in the higher field region suggests that the long-range interaction (mean-field model $\beta = 0.5$ and $\gamma = 1$) is not valid in infinite-layer LSMO. According to the Banerjee's criterion, the positive slope of the line in the Arrott plot corresponds to the second-order phase transition while a negative slope corresponds to the first-order phase transition [49]. Hence, again, the Arrott plot is in agreement with the entropy analysis, Landau analysis and confirms the second-order phase transition in infinite-layer. To determine the appropriate critical exponents (β and γ) and hence universality class to which infinite-layer LSMO might belong, we have focused our attention to the modified Arrott plots (MAPs).

It is widely known that the critical behavior of a system exhibiting a second-order phase transition can be studied with the help of a series of critical exponents (α, β, γ and δ) and different universality classes can be distinguished based on these critical exponents. Also, we know that one cannot discriminate various models based on δ value only because all the universality classes have almost similar values (see table 2). The 3D-Ising model, 3D-XY model, 3D-Heisenberg model, and tricritical mean field model has a δ value 4.82, 4.81, 4.8 and 5 respectively [19, 53, 54]. The appearance of divergence of the correlation length $\xi = \xi_0 |T - T_C/T_C|^{-\nu}$ in the vicinity of the T_C leads to universal scaling laws for the spontaneous magnetization $M_S(T)$ and the initial susceptibility $\chi_0(T)$. According to the universal scaling hypothesis, the mathematical definitions of critical exponents in the vicinity of T_C from magnetization are defined as [44, 50, 51]

$$M_S(T) = M_0(-\epsilon)^{\beta}; \ \epsilon < 0, \ T < T_C, \tag{8}$$

$$\chi_0^{-1} = (h_0/M_0)(\epsilon)^{\gamma}; \ \epsilon > 0, \ T > T_C, \tag{9}$$

and

$$M = DH^{1/\delta}; \ \epsilon = 0, \ T = T_C, \tag{10}$$

Table 2. Comparison of critical exponents β, γ and δ of infinite-layer LSMO with various theoretical models. RG: Renormalization group, CI: Critical isotherm and EA: Entropy analysis.

	Method	T_C (K)	α	β	γ	δ
(Theory)						
Mean field [19, 53]			0	0.5	1	3
Tricritical mean field [19, 54]			0	0.25	1	5
3D-ISing ($d = 3, n = 1$) [19, 53]			0.11	0.325	1.241	4.82
3D-XY ($d = 3, n = 2$) [19, 53]			−0.007	0.346	1.316	4.81
3D-Heisenberg ($d = 3, n = 3$) [19, 53]			−0.115	0.365	1.386	4.8
(Experiment)						
La$_{0.825}$Sr$_{0.175}$MnO$_3$	MAPs	274.11 ± 0.06		0.319 ± 0.001		
		274.02 ± 0.02			1.18 ± 0.03	
	CI					4.67 ± 0.03
	KF	274.16 ± 0.02		0.321 ± 0.003		
		274.13 ± 0.01			1.22 ± 0.01	
	EA	274		0.320 ± 0.020	1.180 ± 0.007	
	RG		0.08	0.34	1.24	4.64

where M_0, M_0/h_0 and D are critical amplitudes. The critical exponents β, γ and δ associated with $M_S(T)$, $\chi_0^{-1}(T)$ and isothermal magnetization at T_C, should follow the Arrott–Noakes equation of state [52] in an asymptotic region $|\epsilon| < 0.1$, expressed as

$$(H/M)^{1/\gamma} = (T - T_C)/T_C + (M/M_1)^{1/\beta}, \qquad (11)$$

where M_1 is the material constant. Finally, the magnetic equation of state is expressed as [44, 53]

$$M(H, \epsilon) = \epsilon^{\beta} f_{\pm}(H/\epsilon^{(\beta+\gamma)}) \qquad (12)$$

where f_+ is defined for $T > T_C$ and f_- is for $T < T_C$. The relation between critical exponents can be given by Rushbrooke and Widom-scaling realtion [50, 54]:

$$\alpha + 2\beta + \gamma = 2, \qquad (13)$$

and

$$\delta = 1 + \frac{\gamma}{\beta}. \qquad (14)$$

Thus, using equations (8), (9) and MAPs ($(M)^{1/\beta}$ versus $(\mu_0 H/M)^{1/\gamma}$), critical exponents β and γ can be obtained by fitting $M_S(T)$ and $\chi_0^{-1}(T)$. While, critical exponent δ can be obtained independently from M-H curve taken at T_C using equation (10).

To construct the MAPs, we have chosen four kinds of possible three dimensional (3D) critical exponents [53, 54] corresponding to 3D-Heisenberg model ($\beta = 0.365$, $\gamma = 1.386$), 3D-Ising model ($\beta = 0.325$, $\gamma = 1.24$), 3D-XY model ($\beta = 0.346$, $\gamma = 1.316$) and tricritical mean field model ($\beta = 0.25$, $\gamma = 1$). All the models for infinite-layer LSMO show quasi-straight lines (figure 6). In this situation, it is difficult to decide the appropriate model to evaluate the critical exponents. In order to determine the appropriate model which describes the system, we have used normalized slope approach. In this method, we have calculated their normalized slopes (NS) which is defined as NS = $S(T)/S(T_C)$, where the slope $S(T) = dM^{1/\beta}/d(\mu_0 H/M)^{1/\gamma}$ (figure 7). If the MAPs

shows a series of parallel lines with the same slope then NS should be 1 regardless of the temperature [55]. It is clear from figure 7 that out of all the models 3D-Ising model is closest to 1 over the temperature range of 262–300 K. On the basis of above analysis it can be emphasized that the exponents β and γ for infinite-layer LSMO may be close to 3D-Ising model. Therefore, we can use the critical exponents of the 3D-Ising model as starting exponents of $M_S(T, 0)$ and $\chi_0^{-1}(T, 0)$ to find out the exact critical exponents of infinite-layer LSMO. In the MAPs of infinite-layer LSMO defined for 3D-Ising model (figure 6(b)), the intercepts with the axes $M^{1/\beta}$ and $(H/M)^{1/\gamma}$ obtained by the linear extrapolation from the high field region yield the reliable values of $M_S(T, 0)$ and $\chi_0^{-1}(T, 0)$. By fitting these values of $M_S(T, 0)$ and $\chi_0^{-1}(T, 0)$ to equation (8) and (9) one set of β and γ is obtained. To find out the exact exponents (β and γ), an iterative method has been used [56]. This process gives the reliable value of critical exponents which are given by: $\beta = 0.319 \pm 0.001$ with $T_C = 274.11 \pm 0.06$ K and $\gamma = 1.18 \pm 0.03$ with $T_C = 274.20 \pm 0.02$ K for infinite-layer LSMO (figure 8(a)).

Again, the critical exponents β and γ can be found more precisely from the Kouvel–Fisher (KF) method [57], given by

$$\frac{M_S(T)}{dM_S(T)/dT} = \frac{T - T_C}{\beta}, \qquad (15)$$

$$\frac{\chi_0^{-1}(T)}{d\chi_0^{-1}(T)/d(T)} = \frac{T - T_C}{\gamma}. \qquad (16)$$

KF method states that $M_S(dM_S(T)/dT)^{-1}$ versus T and $\chi_0^{-1}(d\chi_0^{-1}/d(T))^{-1}$ versus T will result the straight line with slopes $1/\beta$ and $1/\gamma$, respectively and the intercepts on the temperature axis give T_C. The critical exponents (β, γ) and the critical temperature (T_C) obtained from the linear fit of the $M_S(dM_S(T)/dT)^{-1}$ and $\chi_0^{-1}(d\chi_0^{-1}/d(T))^{-1}$ for infinite-layer LSMO are $\beta = 0.321 \pm 0.003$ with $T_C = 274.16$ K ± 0.02 and $\gamma = 1.22 \pm 0.01$ with $T_C = 274.13$ K ± 0.01 (figure 8(b)). One can see that the critical exponents determined from
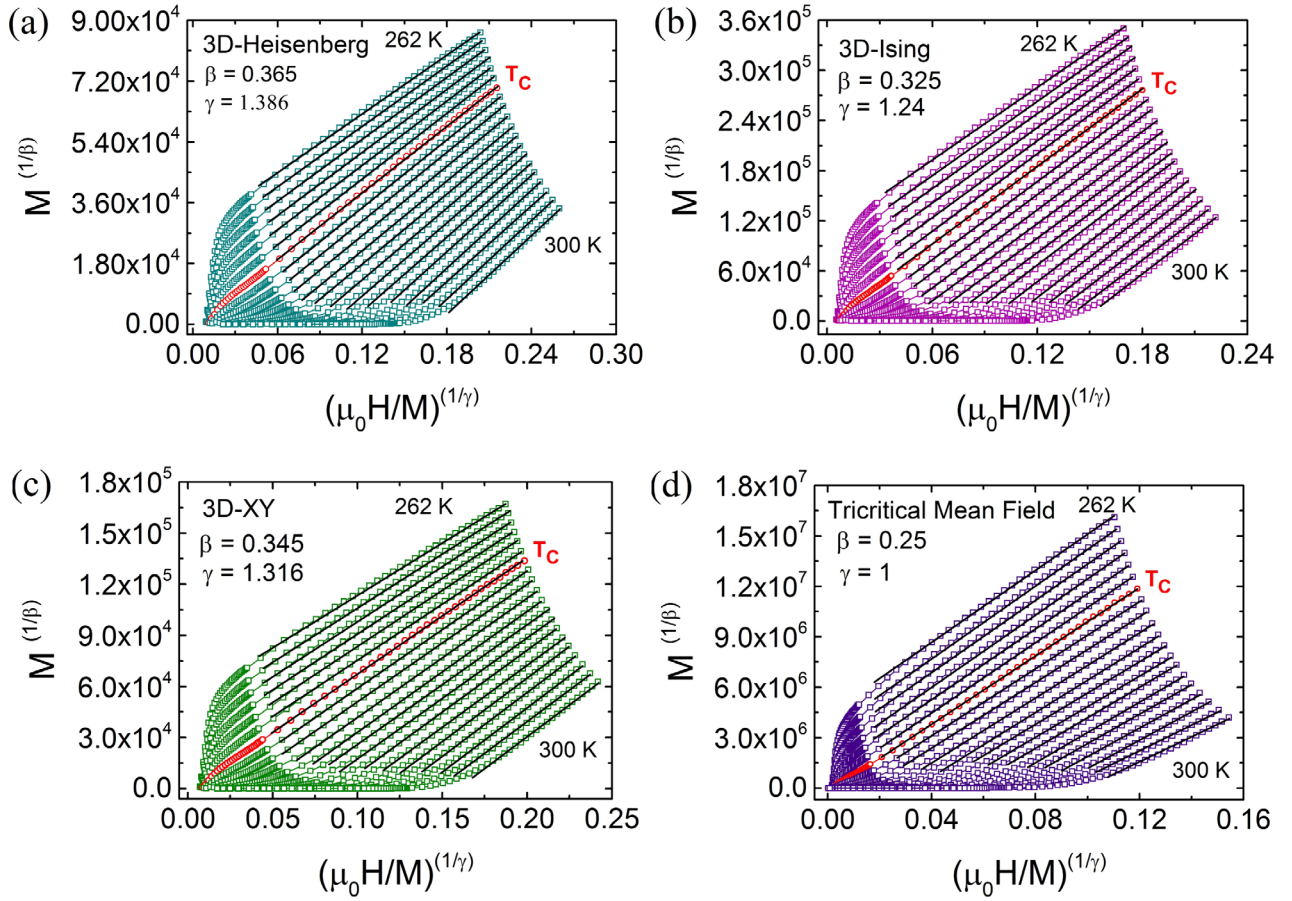
Figure 6. The isotherms of $M^{1/\beta}$ versus $(H/M)^{1/\gamma}$ with (a) 3D-Heisenberg model, (b) 3D-Ising model, (c) 3D-XY model and (d) tricritical mean-field model.
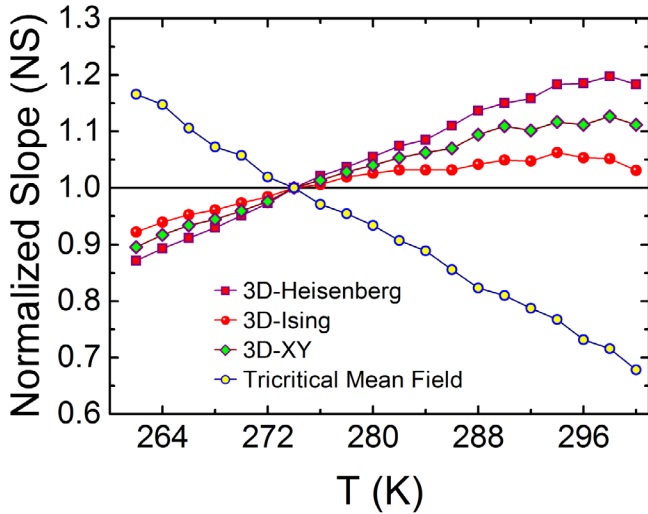

Figure 7. Normalized slopes (NS $= S(T)/S(T_C)$) for different models (3D-Heisenberg, 3D-Ising model, 3D-XY model, tricritical mean field model) as a function of temperature. Where slope $S(T) = dM^{1/\beta}/d(\mu_0 H/M)^{1/\gamma}$, $S(T_C)$ is the slope at T_C.

KF method is in agreement with the exponents obtained from MAPs.

Further, we have used field dependent magnetic entropy change to find out the critical exponents of infinite-layer

LSMO. The field dependence of magnetic entropy change for second-order transition can be expressed as [58]:

$$\Delta S_M = a(\mu_0 H)^b, \tag{17}$$

where b depends on the magnetic state of the sample. The value of b is decided by the linear plot of $\ln(|\Delta S_M|)$ versus $\ln(H)$ at T_C is shown in figure 9(b). The value of b has been found to be 0.547. Now critical exponents are determined using the following relations [58]:

$$n = 1 + \frac{1}{\delta}\left(1 - \frac{1}{\beta}\right), \tag{18}$$

$$n = 1 + \left(\frac{\beta - 1}{\beta + \gamma}\right). \tag{19}$$

The critical exponent δ is determined independently from the critical isotherm at T_C by using equation (10). Figure 9 shows the isothermal M–H at T_C and inset shows linear fit of the log–log plot in the higher field region. Slope of the linear fit of the log–log plot defines $1/\delta$ resulting $\delta = 4.670 \pm 0.030$. Further, critical exponents $\beta = 0.320 \pm 0.020$ and $\gamma = 1.180 \pm 0.007$ are determined by using the equations (18) and (19) respectively. The values of critical exponents (β and γ) match well with the exponents determined by MAPs and KF method.

Finally, the reliability of the exponents β, γ and δ is ensured by Widom-scaling relation [59] using equation (14). Using Widom-scaling relation and the exponents β, γ, obtained from both MAPs and KF method, the δ value for infinite-layer LSMO has been found to be 4.69, 4.80 respectively. Therefore, the critical exponents obtained from both the method are reliable and unambiguous. Further, to check the reliability of the obtained exponents, theory of critical phenomena [44, 53] has been employed by equation (12). If the critical exponents obey this relation then all the data should collapse onto two separate curves below and above T_C in the plot of $M\epsilon^{-\beta}$ versus $\mu_0 H\epsilon^{-(\beta+\gamma)}$ [28, 60]. Figure 10(a) shows the scaling plot of renormalized magnetization, m ($m = M\epsilon^{-\beta}$) and field, h ($h = H\epsilon^{-(\beta+\gamma)}$). All the data collapse onto two independent universal curves above and below T_C. The scaled renormalized magnetization and field confirm the validity of the above analysis. In addition, the reliability of the critical exponents and T_C has been again confirmed more precisely by plotting m^2 versus h/m [53]. One can see that all data collapse onto two separate curves: one below T_C and other above T_C (figure 10(b)). This implies that in critical regime, the interactions get appropriately renormalized following the scaling equation of state.

Further, we have plotted the MAPs for $\beta = 0.321$ and $\gamma = 1.22$ obtained from KF method in very small range $\left(|\epsilon| < 0.03\right)$ near T_C. All the isotherms in MAPs display as closely as possible parallel lines in higher field region, which is shown in figure 11. This is again the validation of our results for infinite-layer LSMO.

3.5. Spin interaction

It is noted that critical exponents obtained for infinite-layer LSMO are different from those of mean field model and tricritical mean field model defined for long-range interaction (see table 2). One can see that exponents of infinite-layer LSMO do not belong to either 3D-XY or 3D-Heisenberg short-range exchange interaction $J(r) \sim e^{-(r/b)}$ (where b is correlation length). The exchange interaction $J(r)$ defines the universality class of the magnetic phase transition for a homogeneous magnet. The interaction between magnetic moments decreases rapidly with distance in short range interaction, while mobile electrons for the itinerant electron system may lead to long range interaction. Fisher *et al* defined a system exhibiting magnetic exchange interaction of the form $J(r) \sim r^{-(d+\sigma)}$ (where d is the dimension and σ is the range of interaction) with the help of renormalization group theory [61]. The analysis suggests that such a model is valid for the value $\sigma < 2$ with long-range interaction. Theoretical models with short-range interaction is only valid for $\sigma \geqslant 2$ and the mean field model explains the critical behavior for $\sigma \leqslant d/2$. The exponent γ can be expressed as follows [61]

$$
\gamma = 1 + \frac{4}{d}\left(\frac{n+2}{n+8}\right)\Delta\sigma + \left(\frac{8(n+2)(n-4)}{d^2(n+8)^2}\right) \\
\times \left[1 + \frac{2G(\frac{d}{2})(7n+20)}{(n-4)(n+8)}\right]\Delta\sigma^2,
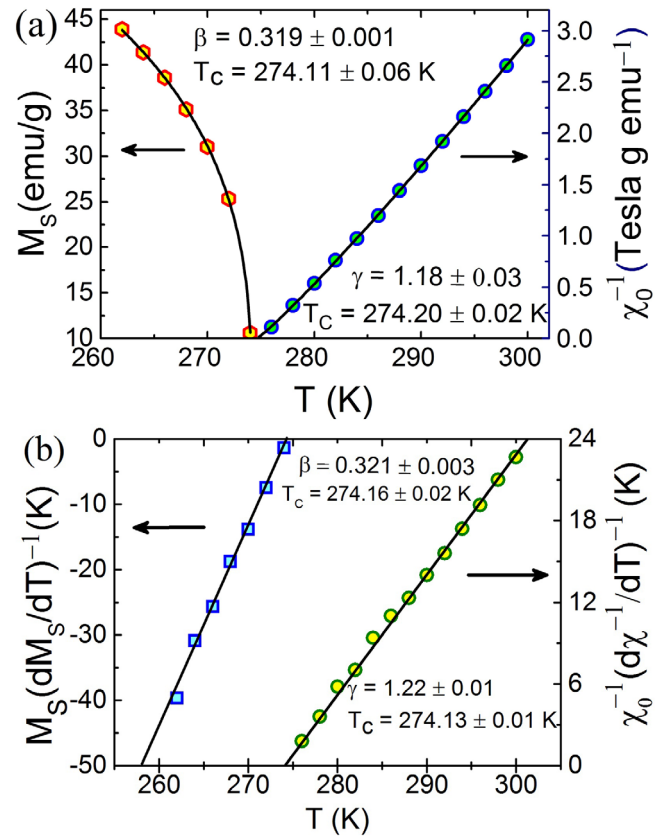\tag{20}
$$

Figure 8. (a) MAPs plots for the Spontaneous magnetization $M_S(T,0)$ (left) and inverse susceptibility $\chi_0^{-1}(T,0)$ (right) as a function of temperature, (b) KF plots for the $M_S(\mathrm{d}M_S(T)/\mathrm{d}T)^{-1}$ (left) and $\chi_0^{-1}(\mathrm{d}\chi_0^{-1}/\mathrm{d}(T))^{-1}$ (right).

where $\Delta\sigma = \left(\sigma - \frac{d}{2}\right)$ and $G(\frac{d}{2}) = 3 - \frac{1}{4}(\frac{d}{2})^2$, n is the spin dimensionality. Above expression holds good for $d/2 \leqslant \sigma \leqslant 2$. We have adopted the method described in [62] to evaluate the range of interaction σ, the dimensionality of both lattice (d) and spin (n). An appropriate value of parameter σ was chosen for a particular values of $\{d : n\}$ so that above expression yield a value of γ close to that of experimentally observed ($\gamma = 1.22$). This process is repeated for different set of $\{d : n\} = \{3 : 1, 2, 3\}$ and yields a value $\sigma = 1.91$ for $\{d : n\} = \{3 : 1\}$, $\sigma = 2.10$ for $\{d : n\} = \{3 : 2\}$ and $\sigma = 2.35$ for $\{d : n\} = \{3 : 3\}$. The value of σ can be used to determine the remaining exponents using following relations: $\nu = \gamma/\sigma$, $\eta = 2 - \sigma$, $\gamma = \nu(2 - \eta)$, $\alpha = 2 - \nu d$, $\beta = (2 - \alpha - \gamma)/2$ and $\delta = 1 + \gamma/\beta$. The sigma value for $\{d : n\} = \{3 : 1\}$ produces $\gamma = 1.24$ with $\beta = 0.34$, and $\delta = 4.64$, which are close to the experimentally observed values of γ, β and δ for infinite-layer LSMO. However, $\sigma = 2.10$ for $\{d : n\} = \{3 : 2\}$ produces $\beta = 0.26$, $\gamma = 1.22$ and $\delta = 5.7$. Similarly, $\sigma = 2.35$ for $\{d : n\} = \{3 : 3\}$ yields $\beta = 0.17$, $\gamma = 1.22$ and $\delta = 8.17$. It can be noted that the obtained critical exponents for the set $\{d : n\} = \{3 : 2, 3\}$ show significant difference from the experimentally determined exponents. Hence, 3D-XY $\{d : n\} = \{3 : 2\}$ and 3D-Heisenberg $\{d : n\} = \{3 : 3\}$ models can be discarded. This implies that the magnetic exchange interaction in infinite-layer LSMO decays as $J(r) \approx r^{-4.91}$. The short-range
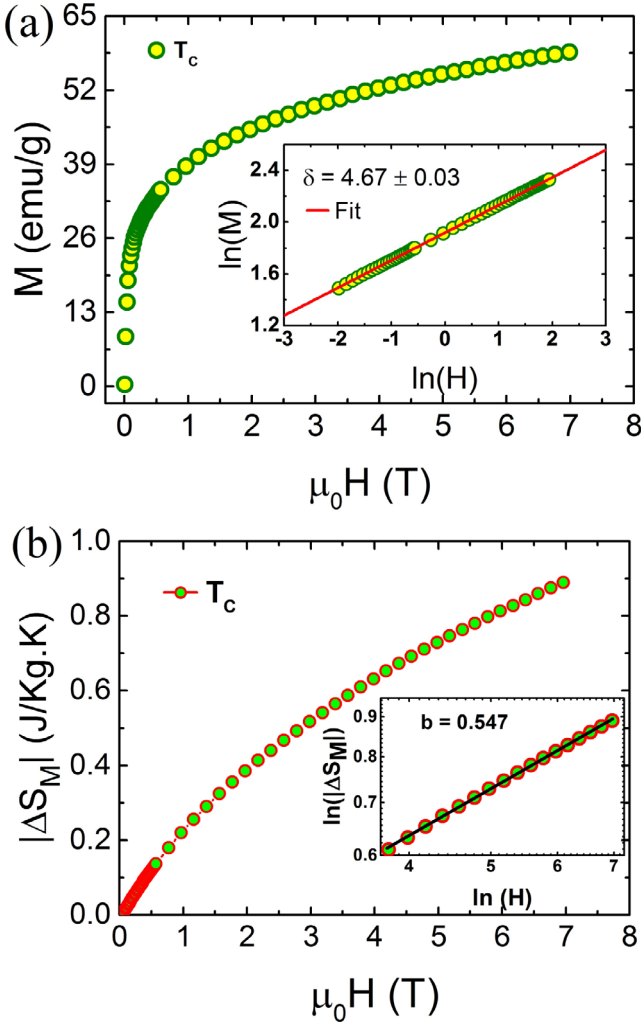
Figure 9. (a) Isothermal M–H plot of infinite-layer LSMO at $T_C = 274$ K. Inset is the log–log plot and the solid line is the linear fit using $M = DH^{1/\delta}$, (b) $|\Delta S_M|$ plot of infinite-layer LSMO at T_C. Inset is the log–log plot and the solid line is the linear fit.

3D-Heisenberg model is valid for $\sigma \geqslant 2$, where $J(r)$ decreases faster than r^{-5}. The mean-field model is satisfied for $\sigma \leqslant 3/2$, resulting slower decrease of $J(r)$ than $r^{-4.5}$. The exponents belong to other universality classes lies in the intermediate range i.e. $3/2 < \sigma < 2$ for which $J(r)$ decreases as $r^{-3-\sigma}$. One can see that σ value for infinite-layer LSMO lies in the intermediate range defined as $3/2 < \sigma < 2$. This confirms that there is short-range magnetic interaction in infinite-layer LSMO. The obtained value of σ for infinite-layer LSMO is then used to find out the other exponents such as $\eta = 0.06$, $\nu = 0.64$, $\alpha = 0.08$. Apart from this, we have also calculated the value of exponent $\alpha = 0.13$ using the Rushbrooke scaling relation defined in equation (13) and exponents β, γ obtained from KF method for infinite-layer LSMO. The exponent α obtained from Rushbrooke scaling relation is close to the value $\alpha = 0.08$ obtained for $\{d : n\} = \{3 : 1\}$ corresponding to 3D Ising system.

All experimental findings discussed in previous sections emphasize that infinite-layer LSMO belongs to the 3D-Ising universality class. Thus, it is clear that magnetic
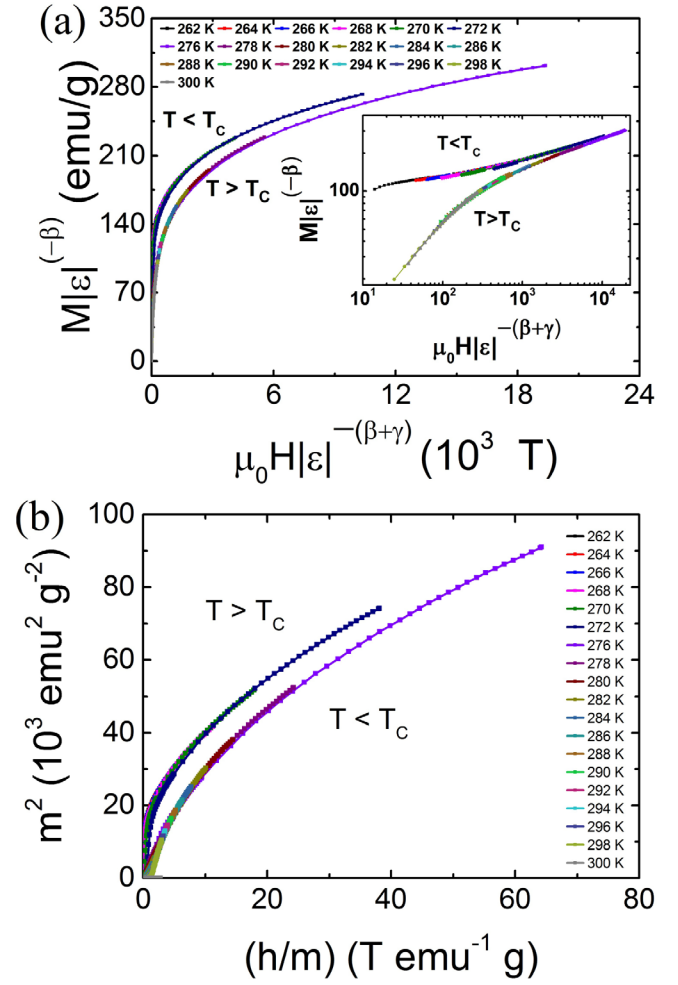

Figure 10. (a) Scaling plots below and above T_C using β and γ determined from Kouvel–Fisher method; the inset shows the same plot in log–log scale, (b) m^2 versus h/m below and above T_C.
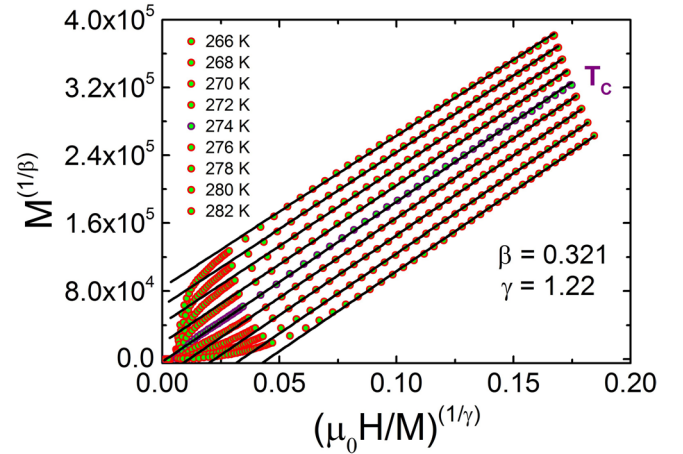

Figure 11. MAPs of infinite-layer LSMO in the range $|\epsilon| < 0.03$ for $\beta = 0.321$ and $\gamma = 1.22$ obtained from KF method in the temperature range 266–282 K.

anisotropy is the leading term in the critical fluctuations in the vicinity of T_C, in opposition to the isotropic exchange mechanism, which is compatible with the 3D-Heisenberg class. The value of the exponent α (=0.08) obtained from our data

is very close to the 3D-Ising universality class. Thus the role of short-range exchange interaction cannot be ruled out in the formation of skyrmions in manganites.

4. Conclusion

In summary, we have investigated the detailed critical behavior of ferromagnetic to paramagnetic phase transition near T_C in the skyrmionic-bubbles host infinite-layer $La_{0.825}Sr_{0.175}MnO_3$ manganite perovskite. Critical exponents β, γ, and δ have been determined by using several methods such as modified Arrott plots (MAPs), Kouvel–Fisher (KF) method, entropy, and critical isotherm analysis. Our result yield short-range 3D-Ising type interaction in $La_{0.825}Sr_{0.175}MnO_3$. Critical exponents obtained from different methods are close to values that define the short-range 3D-Ising universality class. The 3D-Ising universality class emphasizes that the description of the magnetic transition in $La_{0.825}Sr_{0.175}MnO_3$ must consider the existence of magnetic anisotropy. Also, it is noteworthy that the obtained critical exponents are in agreement, with the magnetic equation of state with the curves collapsing onto two separate branches above and below T_C. This conclusively indicates that the obtained critical exponents (β, γ, and δ), as well as critical temperature, are unambiguous and intrinsic to the system. The critical exponents determined from various methods in this study are close to the values calculated from renormalization group approach for 3D-Ising model ($\{d : n\} = \{3 : 1\}$) based on short-range interaction. So, it is necessary to look into whether short-range exchange interaction plays any role in the formation of skyrmionic-bubbles in manganites.

Acknowledgments

ORCID iDs

Subhasis Ghosh ⓘ https://orcid.org/0000-0003-1346-5635

References

[1] Nagaosa N and Tokura Y 2013 *Nat. Nanotechnol.* **8** 899
[2] Fert A, Cros V and Sampaio J 2013 *Nat. Nanotechnol.* **8** 152
[3] Chauhan H C, Kumar B, Tiwari J K and Ghosh S 2019 *Phys. Rev.* B **100** 165143
[4] Yu X, Kanazawa N, Onose Y, Kimoto K, Zhang W, Ishiwata S, Matsui Y and Tokura Y 2011 *Nat. Mater.* **10** 106
[5] Jonker G and Van Santen J 1950 *Physica* **16** 337–49
[6] von Helmolt R, Wecker J, Holzapfel B, Schultz L and Samwer K 1993 *Phys. Rev. Lett.* **71** 2331
[7] Chahara K I, Ohno T, Kasai M and Kozono Y 1993 *Appl. Phys. Lett.* **63** 1990–2
[8] Jin S, Tiefel T H, McCormack M, Fastnacht R, Ramesh R and Chen L 1994 *Science* **264** 413–5
[9] Rao C and Cheetham A 1997 *Science* **276** 911–2
[10] Yu X, Tokunaga Y, Kaneko Y, Zhang W, Kimoto K, Matsui Y, Taguchi Y and Tokura Y 2014 *Nat. Commun.* **5** 3198
[11] Yu X, Tokunaga Y, Taguchi Y and Tokura Y 2017 *Adv. Mater.* **29** 1603958
[12] Mohan C V, Seeger M, Kronmüller H, Murugaraj P and Maier J 1998 *J. Magn. Magn. Mater.* **183** 348–55
[13] Schwartz A, Scheffler M and Anlage S M 2000 *Phys. Rev.* B **61** R870
[14] Lofland S, Ray V, Kim P, Bhagat S, Manheimer M and Tyagi S 1997 *Phys. Rev.* B **55** 2749
[15] Nair S, Banerjee A, Narlikar A, Prabhakaran D and Boothroyd A 2003 *Phys. Rev.* B **68** 132404
[16] Ghosh K, Lobb C, Greene R, Karabashev S, Shulyatev D, Arsenov A and Mukovskii Y 1998 *Phys. Rev. lett.* **81** 4740
[17] Vasiliu-Doloc L, Lynn J, Mukovskii Y, Arsenov A and Shulyatev D 1998 *J. Appl. Phys.* **83** 7342–4
[18] Martin M C, Shirane G, Endoh Y, Hirota K, Moritomo Y and Tokura Y 1996 *Phys. Rev.* B **53** 14285
[19] Kim D, Zink B, Hellman F and Coey J 2002 *Phys. Rev.* B **65** 214424
[20] Oleaga A, Salazar A, Prabhakaran D and Boothroyd A 2004 *Phys. Rev.* B **70** 184402
[21] Lin P, Chun S, Salamon M, Tomioka Y and Tokura Y 2000 *J. Appl. Phys.* **87** 5825–7
[22] Furukawa N and Motome Y 2002 *Appl. Phys.* A **74** s1728–30
[23] Guidi M C, Allodi G, De Renzi R, Guidi G, Hennion M, Pinsard L and Amato A 2001 *Phys. Rev.* B **64** 064414
[24] Oleaga A, Salazar A, Prabhakaran D and Boothroyd A 2005 *J. Phys.: Condens. Matter.* **17** 6729
[25] Fawcett I D, Sunstrom J E IV, Greenblatt M, Croft M and Ramanujachary K 1998 *Chem. Mater.* **10** 3643–51
[26] Fan J *et al* 2019 *Ceram. Int.* **45** 9179–84
[27] Oleaga A, Salazar A, Hatnean M C and Balakrishnan G 2015 *Phys. Rev.* B **92** 024409
[28] Phan M, Franco V, Bingham N, Srikanth H, Hur N and Yu S 2010 *J. Alloys Compd.* **508** 238–44
[29] Kim D, Revaz B, Zink B, Hellman F, Rhyne J and Mitchell J 2002 *Phys. Rev. lett.* **89** 227202
[30] Terashita H, Myer B and Neumeier J 2005 *Phys. Rev.* B **72** 132415
[31] Kotani A, Nakajima H, Ishii Y, Harada K and Mori S 2016 *AIP Adv.* **6** 056403
[32] Dabrowski B *et al* 1999 *Phys. Rev.* B **60** 7006
[33] Franco V, Conde A, Romero-Enrique J and Blázquez J 2008 *J. Phys.: Condens. Matter.* **20** 285207
[34] Romero-Muniz C, Tamura R, Tanaka S and Franco V 2016 *Phys. Rev.* B **94** 134401
[35] Franco V, Conde A, Pecharsky V and Gschneidner K Jr 2007 *Europhys. Lett.* **79** 47009
[36] Bonilla C M, Herrero-Albillos J, Bartolomé F, García L M, Parra-Borderías M and Franco V 2010 *Phys. Rev.* B **81** 224424
[37] Guetari R, Bartoli T, Cizmas C, Mliki N and Bessais L 2016 *J. Alloys Compd.* **684** 291–8
[38] Bingham N, Phan M, Srikanth H, Torija M and Leighton C 2009 *J. Appl. Phys.* **106** 023909
[39] Li R, Tong W, Pi L and Zhang Y 2014 *J. Magn. Magn. Mater.* **355** 276–81
[40] Wali M, Skini R, Khlifi M, Dhahri E and Hlil E 2015 *Dalton Trans.* **44** 12796–803
[41] Phan M H, Yu S C and Hur N H 2005 *Appl. Phys. Lett.* **86** 072504
[42] Bhattacharyya A, Chatterjee S, Giri S and Majumdar S 2009 *Eur. Phys. J.* B **70** 347–51
[43] Guo Z, Du Y, Zhu J, Huang H, Ding W and Feng D 1997 *Phys. Rev. lett.* **78** 1142
[44] Stanley H E 1999 *Rev. Mod. Phys.* **71** S358

[45] Widom B 1965 *J. Chem. Phys.* **43** 3898–905
[46] Xu L, Fan J, Zhu Y, Shi Y, Zhang L, Pi L, Zhang Y and Shi D 2016 *Mater. Res. Bull.* **73** 187–91
[47] Shimizu M 1981 *Rep. Prog. Phys.* **44** 329
[48] Arrott A 1957 *Phys. Rev.* **108** 1394
[49] Banerjee B 1964 *Phys. lett.* **12** 16–7
[50] Stanley H E 1971 *Phase Transitions and Critical Phenomena* (Oxford: Clarendon)
[51] Fisher M E 1967 *Rep. Prog. Phys.* **30** 615
[52] Arrott A and Noakes J E 1967 *Phys. Rev. Lett.* **19** 786
[53] Kaul S 1985 *J. Magn. Magn. Mater.* **53** 5–53
[54] Huang K 1987 *Statistical Mechanics* (New York: Wiley)

[55] Fan J, Ling L, Hong B, Zhang L, Pi L and Zhang Y 2010 *Phys. Rev. B* **81** 144426
[56] Zhang L, Fan J, Zhu X, Ning W, Qu Z, Ge M, Pi L and Zhang Y 2013 *Appl. Phys. A* **113** 201–6
[57] Kouvel J S and Fisher M E 1964 *Phys. Rev.* **136** A1626
[58] Franco V, Blázquez J and Conde A 2006 *Appl. phys. lett.* **89** 222512
[59] Kadanoff L P 1966 *Phys. Phys. Fiz.* **2** 263
[60] Khan N, Midya A, Mydeen K, Mandal P, Loidl A and Prabhakaran D 2010 *Phys. Rev. B* **82** 064422
[61] Fisher M E, Ma S K and Nickel B 1972 *Phys. Rev. Lett.* **29** 917
[62] Fischer S, Kaul S and Kronmüller H 2002 *Phys. Rev. B* **65** 064443